Deutscher Luft- und Raumfahrtkongress 2008
DocumentID: 81306

PREDICTION OF TURBINE ROTOR BLADE FORCING DUE TO IN-SERVICE STATOR VANE TRAILING EDGE DAMAGES

M. Meyer, R. Parchem, P. Davison, Rolls-Royce Deutschland, Germany.

Abstract
This paper gives an overview of the current (mid-term) status of the project "Analyse von Betriebsschäden", funded by the German Aeronautical Research Program, Phase IV (LuFo IV), whose objective is the assessment of the influence of damaged high pressure turbine nozzle guide vanes onto the low engine order excitation of the downstream rotor blade. To quantify the forcing, the modal forces for the rotor eigenmodes of interest are obtained by solving the instationary Navier-Stokes equations for a full assembly of stator and rotor ring. Since the computing resources for such a calculation are too high to be routinely employed for the assessment of in-service damage patterns, the approach chosen is to perform a sufficient number of forced response calculations with different damage patterns in advance and use the results to build a surrogate model that will be used to assess the severity of damage patterns by simple interpolation. The focus of this paper thus lies on (i) parameterization of the damage, (ii) the process to automatically perform a large number of forced response calculations and (iii) the chosen surrogate model.

1. INTRODUCTION

During the operation of jet engines it is possible that damages occur on the trailing edges of the high pressure turbine nozzle guide vanes (NGVs), see fig. 1: Due to the extremely high temperatures in this region of the engine, which on average exceed the melting temperature of the employed vane material by more than 300 degrees during takeoff, any unintended decrease of the vane cooling mass flow can lead to a loss of trailing edge material. The structure of the NGV can withstand a significant amount of trailing edge material loss, thus posing no imminent threat to the engine. But additionally the damage changes the flow through the affected passage, causing a so-called low engine order excitation of the rotor blades downstream [1]. During normal operation of the engine a small amount of low order excitation is present due to allowable tolerances in the static components, but extreme cases of throat width variation can lead –in extreme cases– to high cycle fatigue failure of the rotor blade, due to resonances in the operating range, as seen in the Campbell diagram in fig. 2. Thus it is very important to be able to quantify the damage-induced rotor forcing in case a trailing edge damage is detected during routine engine inspection. This quantification can be obtained by solving the unsteady flow for a full NGV and rotor ring, typically modeled using the Reynolds-averaged Navier-Stokes equations together with a suitable turbulence model. The rotor forcing is then obtained by projecting the instationary rotor blade pressure onto the rotor eigenmodes of concern. Due to the large mesh that is required (approximately 30 million grid points) and the low frequency contents that need to be resolved, such a flow calculation requires currently around 2 weeks on 40 processors. This is clearly too time and CPU-resource consuming for routine use. On the other hand a growing fleet of engines that enter service necessitate the capability of quick assessment of in-service damage patterns. In order to facilitate the desired quick response times in the order of at most several hours, the following approach has been chosen: Using a suitable parameterization of the shape of the individual trailing edge damages and of the distribution of those damages over the circumference of the NGV ring, a customized design-of-experiment matrix is set up with a suitably high number of damage shapes. For those specified designs the forced response calculation is performed offline. The resulting forcing values are used to build an interpolating surrogate model which can be employed to assess future in-service damage patterns without the need to resort to lengthy CFD computations. In the following paragraphs this solution approach will be described in more detail: First the parameterization of the damage shape will be described. The next section details the generation of a customized design-of-experiments matrix. Then the process employed to automatically perform the required forced response calculations is described. In the last section the first results of forced response calculations will be discussed.

2. DAMAGE PARAMETERIZATION

If one employs a general approach for the parameterization of the individual damage shape, for example by using a spline with 5 control points, the resulting dimension of the design-of-experiment (DOE) would lie in the order of 400 degrees of freedom. For a reasonably accurate response surface we should allow at least 5 points per degree of freedom. This would lead to 2000 required forced response calculations, each of which needs 2 weeks on 40 processors to complete. This is far too resource consuming even on a very large high-performance computing cluster. Thus the need to reduce the dimensionality of the problem as much as possible is clearly evident. In the following sections we describe the approximations employed to obtain a manageable small number of free variables for the resulting design-of-experiment.

2.1. Parameterization of individual damage shapes

Inspection of available pictures of trailing edge damages of the engine in question suggests that the individual damage can be approximated well by a trapezoidal shape, as shown in fig. 1: It is possible to describe the individual damage shape reasonably with five parameters, the damage width at trailing edge (w_1) and damage front (w_2) as well as the damage depth (d) and the mid-point heights (h_1, h_2), as shown in fig. 1. But even with five parameters per damage shape the resulting number of degrees of freedom would be 200, since there are 40 NGVs present in the assembly under study. This dimension is too high, thus –in order to reduce the dimensionality further– a statistical analysis of all available trailing edge damage shapes has been carried out: All available damage shapes have been approximated by trapezoids, i.e. the parameters w_1, w_2, h_1, h_2 and d have been calculated for each shape. The results of this analysis were (i) that the damage is mostly centered at mid-span, i.e. $h_1 = h_2$ = 50% height, as seen in the histograms depicted in figure 3, and (ii) that there exists a correlation between damage area and the other three parameters: When the obtained values for w_1, w_2 and d are plotted over the damage area, as shown in figures 4 to 6, a high degree of correlation is evident for the parameters w_1 and d: They can be approximated with the cubic functions shown in figure 4 and 5 with adjusted correlation coefficients of r_{w1}=0.74 and r_d=0.87 respectively, i.e. there exists a statistically significant correlation. The third parameter w_2 on the other hand shows a more random behavior. Nevertheless it was decided to also approximate the parameter w_2 with a cubic function as shown in figure 6, even if the correlation coefficient of this approximation is only r_{w2}=0.46. This enables us to deduce the damage shape from a single value, the prescribed damage area, thus reducing the number of free parameters per NGV to only one. Several examples of the damage shapes generated by the curve approximations to w_1, w_2, d and $h_1 = h_2$ = 50% are shown in figs. 7 and 8. The number of free parameters for the design-of-experiment is now equal to the number of NGVs, i.e. 40 in our case.

2.2. Generation of the design-of-experiment matrix

The free parameters of our DOE setup are the damage areas of the 40 individual NGVs, where the area value a is defined as the amount of missing area expressed as percentage of the total area, given by the product of true chord and mean radial height of the NGV. The upper bound of the damage area was chosen to be 15%, based on the results of the statistical analysis above. In order to limit the number of meshes that have to be generated for the damaged NGVs, 7 discrete levels of damage were selected with a = [0%, 2.5%, 5%, 7.5%, 10%, 12.5%, 15%] damage area. Some examples of the associated damage shapes are shown in fig. 8.

To further reduce the dimensionality of the problem, the circumferential variations from the flow disturbances upstream of the NGV will be neglected, thus making the assembly under consideration rotationally symmetric: Any duplicate of a damaged NGV assembly that is created by rotating the NGV ring by an integer multiple of the pitch angle will yield the same forcing on the following rotor ring as the original non-rotated assembly. This fact fortunately reduces the required number of designs significantly, since each design site introduces all its rotated copies into the design matrix without the need to perform individual forced response calculations of these rotated copies. This will be exploited in the setup of the design-of-experiment matrix as follows: The design-of-experiment matrix will be built up from three parts: The first design sites are selected to be the single NGV damage cases of the prescribed levels a_i since those single damage cases are believed to occur most frequently during operation. The second set of design sites are selected to be those cases that excite a pure engine order frequency in the engine operating range, which will lead to a resonance of the first flap mode, i.e. the worst case scenario. From the Campbell diagram in fig. 2 it can be seen that in our case the 7th engine order up to the 12th engine order need to be considerd. Those pure engine order excitation cases are created by placing [7, 8, ...,12] NGVs with damage level a_7 as equally as possible on the circumference of the NGV ring. The third set of 30 additional design points are chosen in such a way to evenly fill the design space (space-filling design). This can been achieved by using a simulated annealing optimization algorithm as described in [6]: Starting from an initial latin hypercube design, the algorithm iteratively seeks to improve the space filling criterion, in our case the maximization of the minimal distance (maximin criterion) found between all possible combinations of design sites. It selects those design sites that exhibit the minimal distance and perturbs randomly selected entries of the corresponding design vectors. In our case the algorithm operates on the full set of 7+6+30 designs, and the minimum distances are evaluated also for all rotated copies of all design sites in order to take the cyclic symmetry into account. The algorithm is allowed to change only the last 30 entries in order to preserve the first two sets of the design matrix. The optimization is repeatedly started from different randomly generated initial latin hypercube designs and the best solution found after 10 trials is selected as design matrix. If the rotational symmetry is taken into account, the 43 designs of the optimal design matrix represent a total of 1620 designs including the rotated copies, i.e. approximately 40 designs per degree of freedom. This number of points should be sufficient for the generation of an interpolating surrogate model.

3. FORCED RESPONSE ANALYSIS: SOLUTION METHODOLOGY

The results presented in this paper are obtained using the Rolls-Royce proprietary code AU3D, an unsteady flow and aeroelasticity solver [2,3] which is based on unstructured meshes [5], thus offering high flexibility for modeling complex geometric shapes. The code solves the Reynolds-averaged Navier-Stokes equations with Spalart-Allmaras turbulence model and has been tested on a wide range of turbomachinery flows [4]. The structural part of the solver employs a modal model obtained from a 3D finite element representation of the rotor blade, see fig. 9. The structural mode shapes, for example the first bending mode which is also shown in fig. 9, are then interpolated onto the fluid mesh. During the instationary computations the structural and fluid boundary conditions, i.e. displacements and pressures, are exchanged at every time step. Although the solver permits movement of the fluid mesh to represent the instantaneous shape and position of the structure undergoing deformation under the influence of the fluid forces, the forced response calculations described in this paper are performed without mesh motion. This reduces computing time and allows the computation of the forces acting on several modes and nodal diameters at once. This feature is especially important since we do not know in advance which nodal diameter and mode shape is excited most by the randomly damaged assemblies. The limit cycle displacements for each mode and nodal diameter are obtained in a post-processing step from the computed modal force time histories.

3.1. Grid generation

The assembly studied in this paper is representative of modern high-pressure turbine (HPT) assemblies. The NGV blade row has 40 vanes, and the following row consists of 74 rotor blades. Both blade rows are cooled, but the details of the cooling flow were omitted in this study to reduce the computational effort. The numerical grids used for NGV and rotor blade row are hybrid meshes, consisting of hexahedral elements in the boundary layer and prismatic elements in the rest of the passage, see fig. 10. The grid sizes of a single NGV and rotor blade passage are 260k points and 240k points, respectively. The meshes are unstructured in the blade-to-blade plane and the 3D grid is obtained by sweeping the unstructured mesh along the blade span [5]. The radial distribution of grid layers and the parameterization of the unstructured mesh follows the recommendations of a mesh refinement study [7], undertaken to find economic meshes of high accuracy.

3.2. Forced response calculation

In the calculation process, schematically depicted in fig. 11, the first step consists in generating single passage NGV meshes for all damage levels and solving the steady flow of these single passage NGV-only setups. In the next step the NGV rings for all design-of-experiment sites are created by automatically assembling undamaged and damaged NGVs into a full assembly according to the given design vector. Additionally a single rotor passage with periodic boundary conditions is placed downstream of the NGV ring. This setup is solved until a steady flow state is reached which yields the initial flow solution for the following time-accurate flow forced response calculation, where the full NGV ring is connected to the full ring of rotor blades. Here the flow equations are advanced in time using second-order accurate implicit time integration with a constant time step that resolves the passing of one NGV pitch with 150 time steps. After each time step the current static pressure on the rotor blades is projected onto all specified mode shapes and nodal diameters to yield the modal forces. (The nodal diameter denotes the number of vibration cycles around the circumference of the rotor ring.) As can be seen from the Campbell diagram in fig. 2, low engine order resonances are expected to occur for the engine orders from 7 to 12. Ideally, a separate forced response calculation should be carried out to assess the resonance at the different speeds with the correct flow boundary conditions, but in order to reduce computational cost, the forced response analysis will only be carried out at 90% speed. The levels of forcing will then be rescaled to the appropriate resonance speeds using the turbine inlet pressure as described in [8]. After the forced response calculations are finished, we thus have obtained the modal force amplitude for each nodal diameter which will be used to build a surrogate model, as described in the next section.

3.3. Surrogate model generation

Surrogate models, also called meta models or response surfaces, can be subdivided into approximating and interpolating models. The approximating models are chosen when the output to be modeled contains random errors, for example when the results are obtained by performing measurements in the laboratory. In our case the results are obtained by performing computer experiments, and the result depends deterministically on the input parameters: If the same input parameters, i.e. damage areas for the NGVs in the assembly, are used for two forced response calculations, both will exhibit the same resulting modal force amplitudes. Thus in the case of computer experiments an interpolating model is the better choice. For scattered data points in a high-dimensional space, the interpolating surrogate models most often employed are radial basis functions (RBF) [9], kriging [10] and neural networks [11]. Since in our case the number of interpolations points (1620) and the dimension of the problem (40) are quite high, the optimization steps in both the kriging and neural network approach can be very time consuming. Thus we will start with a radial basis function model and check the approximation quality using the cross validation technique. For the radial basis function model, the user has to specify the kind of basis function to use and the degree of the polynomial for the approximation of the global trend. The correct choices are not obvious and differ from application to application. Thus we will fit RBF models for all possible combinations of basis function and polynomial degree, evaluate the goodness of fit by performing a cross validation for each model and then select that model which displays the lowest error. The cross validation is performed by randomly removing an entry from the design matrix, rebuilding the RBF model with the reduced set of design points, then comparing the interpolated value obtained from the RBF model for the removed data point with the actual, known value, thus obtaining an error measure. This is repeated several, in our case 10 times, and the final root-mean-square value of the relative error is used to select the best model for our application.

4. RESULTS

Due to the very high computational effort involved in this study, not all forced response calculations of the specified design-of-experiment matrix have been finished yet, thus we will only report preliminary results in this paper. In the following section the steady flow solution around a level-7 damaged vane will be examined in closer detail in order to obtain a better understanding of the damage-induced flow distortions. The next section describes the analysis of the frequency content of the total pressure variation in circumferential direction of the steady full NGV ring+single rotor passage setup. This will be a good indicator of the engine order excitations that can be expected in the forced response calculations that follow and can serve as a test of the surrogate model generation algorithms, as described in the following paragraph. The last section reports first results of the forced response calculations.

4.1. Steady flow solution around a vane with trailing edge damage

For the calculation of the steady flow, prescribed values for total temperature, total pressure and flow angles where used as inflow boundary conditions and static pressure was prescribed as exit boundary condition downstream of the rotor. The interface between the full NGV assembly and the rotor passage is modeled as a mixing plane. In fig. 12 the absolute Mach number is shown for an NGV with level-7 damage inserted into an otherwise undamaged assembly. We see two strong vortices forming at the edges of the damage and an increase in velocity on the leading edge suction side region of the undamaged counterclockwise adjacent vane. Those damage-induced vortices lead to a significant change of the NGV wake, which can be seen in fig. 13, where the total pressure is shown in the NGV exit plane. The vortices additionally distort the wakes of the two adjacent vanes, but the distortions are restricted to the wake region plus and minus one pitch around the damaged vane position.

4.2. Fourier decomposition of the total pressure in the NGV exit plane

In order to obtain a first impression of the engine order excitations that can be expected in the following forced response analysis, the circumferential frequency content of the total pressure in the NGV exit plane of the steady flow solution has been analysed: For each radial grid layer a Fourier decomposition based on multiples of the engine rotation frequency has been carried out and area-averaged over the radial height to yield the final EO contents as displayed in fig. 14: Here the engine order decomposition for all designs is shown in one plot. The *x* axis corresponds to the individual design number and the *y* axis denotes the multiple of the engine order. On the *z* axis the amplitude of the individual Fourier components are plotted. The first design is the undamaged reference case, the following assemblies are the 43 cases specified by the optimal design-of-experiment matrix. It can be seen that the energy is redistributed from the main excitation (40^{th} engine order due to the number of NGVs) to lower engine orders for all damaged cases. The amount of redistribution correlates with the amount of damage area present in the assembly with the worst case being the purely 12^{th} engine order excitation assembly. Thus we expect the maximal forcing to occur for this design and that the 12^{th} nodal diameter assembly modeshape will be excited . It is interesting to note that the relation between 40^{th} engine order content and damage area is linear for the single damage cases and also all pure EO cases, as can be seen in fig. 14 and more clearly in fig. 15. Both sets consist of damaged NGVs that are surrounded by undamaged NGVs, i.e. the flow of the damaged assembly can be seen as a superposition of wakes from damaged and undamaged NGV wakes stitched together.

4.3. Surrogate model generation

Since the forced response calculations are not finished yet, the Fourier decomposition of the total pressure in the NGV exit plane as shown in fig. 14 can be used to demonstrate the surrogate model generation process. We have chosen the radial basis function model as interpolating surrogate model, since this model can be generated efficiently for the large number of design points and the high dimension of the problem and does not (in contrast to for example the Kriging model) involve an optimization step. In order to find the correct basis function and polynomial degree for the application at hand, we perform a 10-trial cross validation for RBF models with all possible combinations of available basis function {thin plate spline, multiquadric, inversemultiquadric, linear, gaussian, cubic} and polynomial degree {0,1,2} and compare the relative root mean square (RMS) error, depicted in fig. 20. (Since all RBF models with a polynomial degree 2 did exhibit a significantly higher error, they have been omitted from figure 20.) It can be seen that the influence of Kernel and degree of polynomial on the RMS error is not very high, all models exhibit a relative error of around 15%. This result carries over to different engine orders, as for example the 12^{th} engine order, where the relative error is approximately 11%. To improve the accuracy of the surrogate model, additional points can be added to the Design-of-Experiments matrix to improve the space-filling property. Another approach would be to employ a Kriging surrogate model, which can be thought of as an RBF model that has been optimized to obtain a lower RMS error. Both options shall be investigated in the future.

4.4. Low engine order excitation – first results

Due to the very high computing resources required for theses calculations, only a limited number of designs have been calculated so far. These preliminary results will be presented in the following. To assess the modal forces for the low engine order excitation, the forced response analysis was carried out for 3500 time steps. Thus the modal force time history contains 4 cycles of the lowest (7^{th}) engine order of interest, from which only the two last cycles will be used for the spectral analysis of the frequency content. In fig. 17 the modal force of the 4^{th} mode / 34^{th} nodal diameter (ND) are compared for an undamaged assembly (design 0) and a randomly damaged assembly (design 43). Mode 4/ND 34 corresponds to the main engine order excitation of the assembly, i.e. the 40^{th} engine order excitation that has been aliased back to the 34^{th} nodal diameter pattern by the number of rotor blades, 34=mod(74,40). It can be seen that the amplitude of this excitation is lower for the damaged assembly, thus energy is redistributed to other frequencies, for example the mode 1/ND 7 excitation, which is shown in fig. 18. This excitation is not present in the undamaged assembly at all, but shows a significant modal force content for the damaged assembly. Which nodal diameter is excited the most depends on the frequency content of the flow and thus on the circumferential distribution of the damaged vanes. For the assembly depicted in fig. 16 (design 43) for example the highest excitation is obtained for the 8^{th} nodal diameter, as can be seen in fig. 19, where all low nodal diameter excitations of interest are compared.

5. CONCLUSIONS AND FUTURE STEPS

In this paper the low engine order excitation of a high pressure turbine rotor blade due to damaged NGV trailing edges has been analysed with the aim to generate a surrogate model for the quick assessment of damage severity. Due to the very high computing resources that are required for the analysis of low engine order excitations, the dimensionality of the design space has to be reduced as much as possible, which has been accomplished by a suitable parameterization of the damage shape, based on a statistical analysis. The process to generate a customized optimal design-of-experiment matrix that takes into account the rotational symmetry of the problem has been described. Since the analysis of low engine order excitations has not been finished yet, preliminary results based on an analysis of the engine order content of the total pressure in the NGV exit plane have been used to demonstrate the generation of the RBF surrogate model and to investigate the approximation quality of the RBF model. It was shown that the approximation of engine order content exhibits an error of approximately 15%. Thus the future steps will be to reduce this error by placing additional points at carefully selected design sites and by employing optimization-based surrogate models like Kriging. Additionally the sensitivity of modal force to the shape parameterization will be investigated to obtain an indicator of the error and possibly corrections factors to account for the approximation of the individual damage shape by the simplified regression-based trapezoidal shape.

6. ACKNOWLEDGEMENTS

The funding of this work under LuFo IV, Call I, Project RobusTurb, contract number 20T0608A by the federal German ministry of economy is gratefully acknowledged. In addition the authors want to thank Dr. di Mare, Imperial College, London, for many helpful discussions and advice.

7. REFERENCES

[1] Breard,C., Green, J.H., Imregun,M.: *Low-engine-order excitation mechanisms in axial-flow turbomachinery*. Journal of Propulsion and Power, Vol. 19, No. 4, pp. 704-712, (2003).

[2] Sayma, A.I., Vahdati, M., Sbardella, L., Imregun, M.: *Modeling of three-dimensional viscous compressible turbomachinery flows using unstructured hybrid grids.* AIAA Journal, Vol. 38, No. 6, pp. 945-954, (2000).

[3]Vahdati, M., Sayma, A.I., Imregun, M.: *An integrated nonlinear approach for turbomachinery forced response prediction. Part I: Formulation. Fluids and Structures.* Vol. 14, No. 1, pp. 87-101, (2000).

[4]Vahdati, M., Sayma, A.I., Imregun, M.: *An integrated nonlinear approach for turbomachinery forced response prediction. Part II: Case studies.* Fluids and Structures, Vol. 14, No. 1, pp. 103-125, (2000).

[5] Sbardella,L., Sayma, A.I., Imregun, M.: *Semi-structured meshes for axial turbomachinery blades.* International Journal for Numerical Methods in Fluids, Vol. 32, No. 5, pp. 569-584, (2000).

[6] Husslage, Bart, Rennen, Gijs, van Dam, Edwin and den Hertog, Dick, *Space-Filling Latin Hypercube Designs for Computer Experiments".* Available at SSRN: http://ssrn.com/abstract=895464, *(March 2006)*

[7] Popig, F.: *Numerische Analyse der Strömung in einer Statorpassage mit beschädigter Hinterkante.* Studienarbeit, Technische Universität Cottbus, (2008).

[8] Green,J.S., Fransson,T.: *Scaling of Turbine Blade Unsteady Pressures For Rapid Forced Response Assessment*, GT2006-90613, Proceedings of the ASME TurboExpo, (2006).

[9] M. J. D. Powell: *Radial basis functions for multivariable interpolation: A review*. Algorithms for approximation, Clarendon Press, pp 143 – 167, (1987).

[10] Stein, M.L.: *Interpolation of Spatial Data: Some Theory for Kriging*, Springer Series in Statistics, (1999).

[11] Poggio, T. Girosi, F.: *Networks for approximation and learning*. Proceedings of the IEEE, Vol. 78, No. 9, pp. 1481-1497, (1990).

8. FIGURES

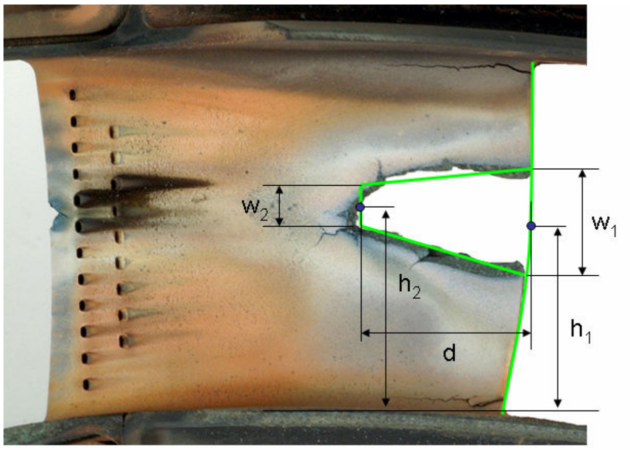

Fig. 1: Nozzle guide vane with trailing edge damage and shape parameterization.

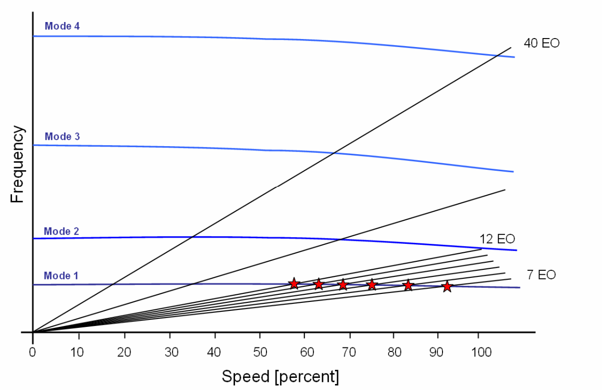

Fig. 2: Example of a Campbell diagram with resonances due to low engine order excitation

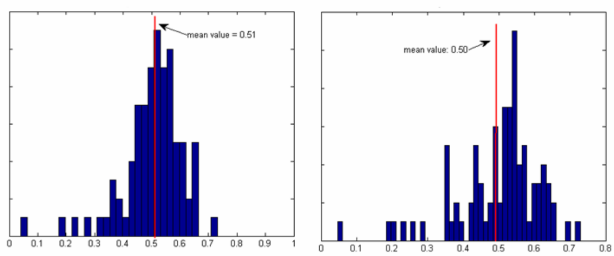

Fig. 3: Histogram of parameter h_1 (left) and h_2 (right).

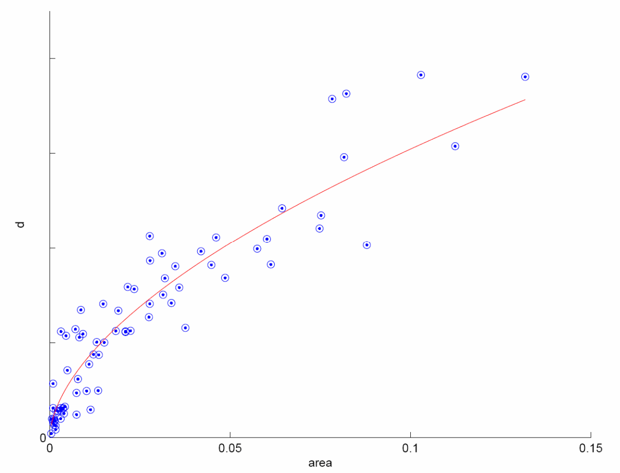

Fig. 4. Damage depth over area and employed regression curve.

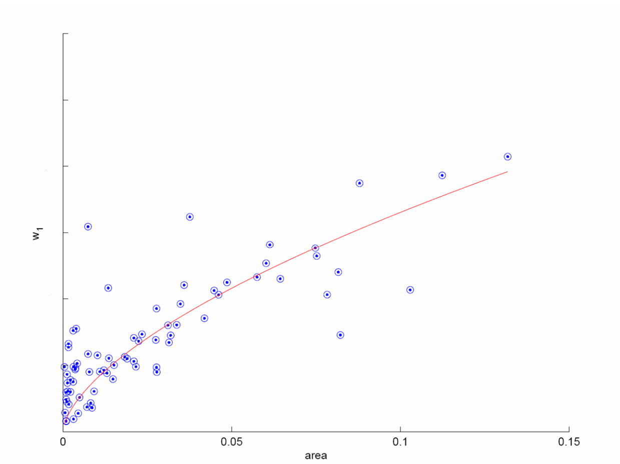

Fig. 5. Damage width at trailing edge over area and employed regression curve.

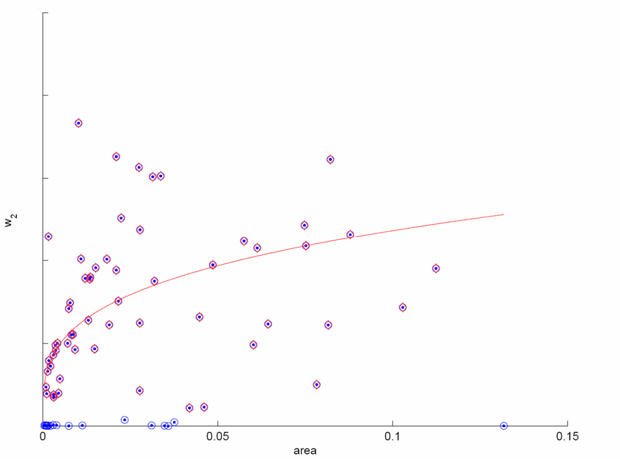

Fig. 6. Damage width at damage front over area and employed regression curve.

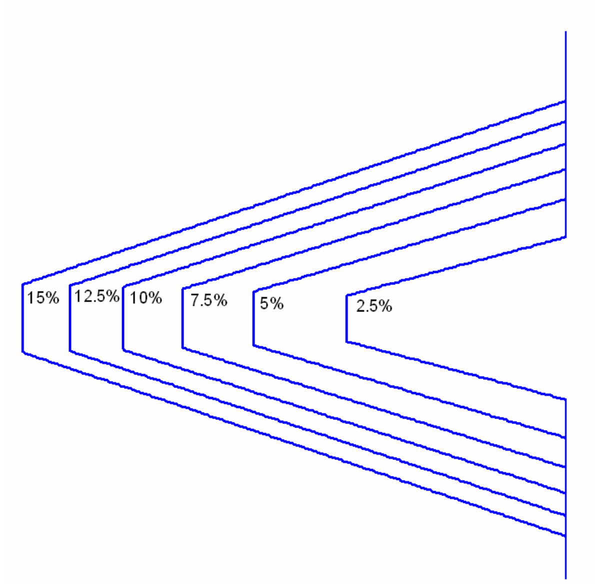

Fig. 7: Damage shapes of selected area levels based on regression analysis.

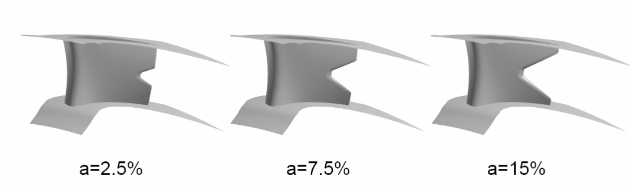

Fig. 8: 3D-view of selected damage levels

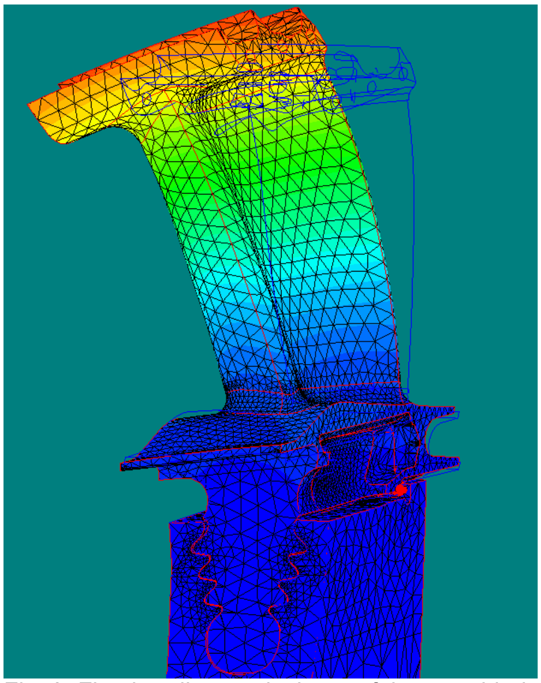

Fig. 9: First bending modeshape of the rotor blade

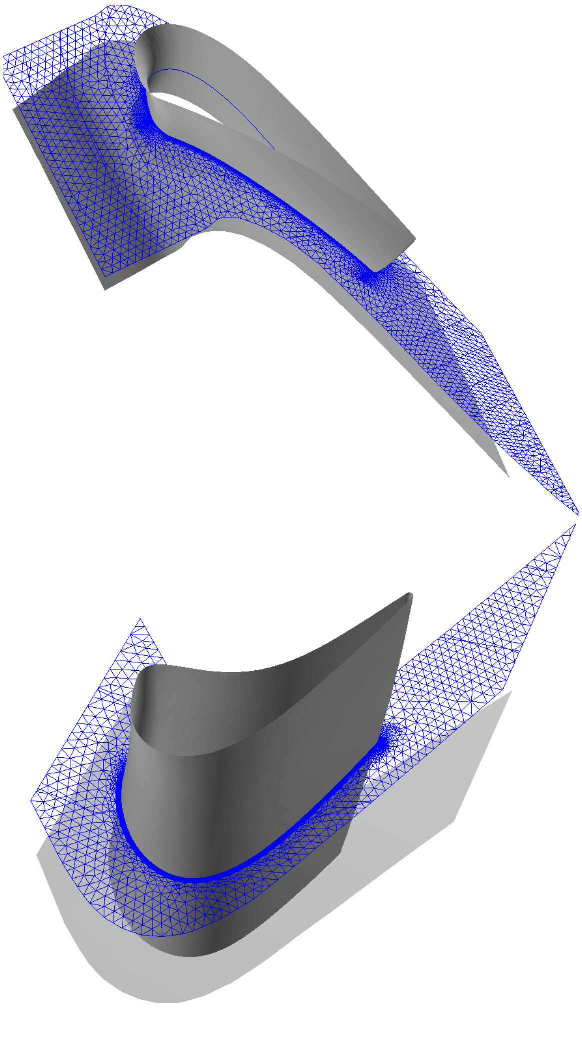

Fig. 10: 2D cut through meshes of undamaged NGV (top) and rotor blade (bottom)

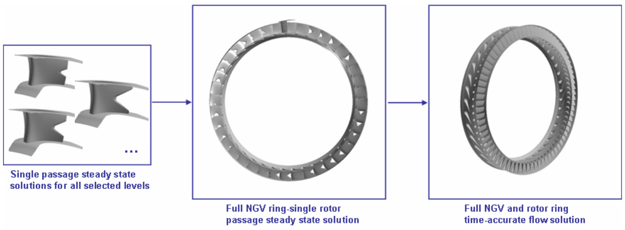

Fig. 11: Flow solutions involved in the calculation process for each design-of-experiment point

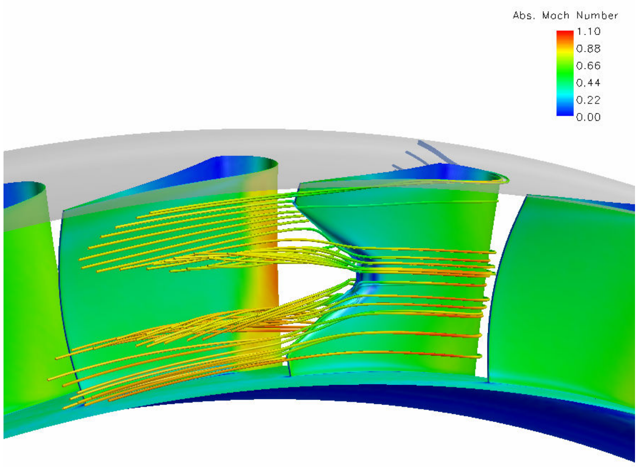

Fig. 12: Vortex formation at edges of a level-7 damaged NGV

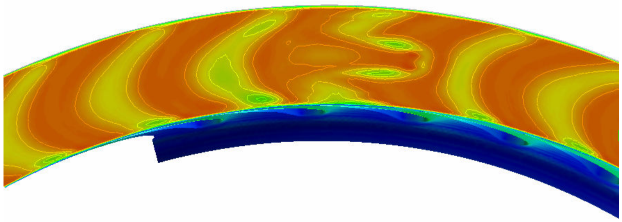

Fig. 13: Total pressure deviation in the wake of a level-7 damaged NGV

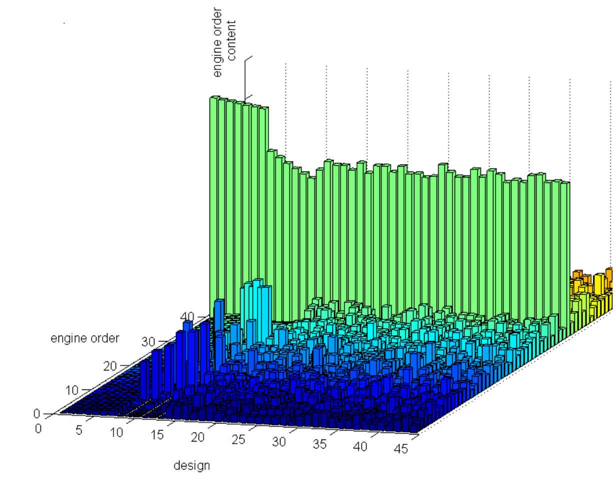

Fig. 14: Circumferential Fourier decomposition of total pressure in the NGV exit plane for all designs

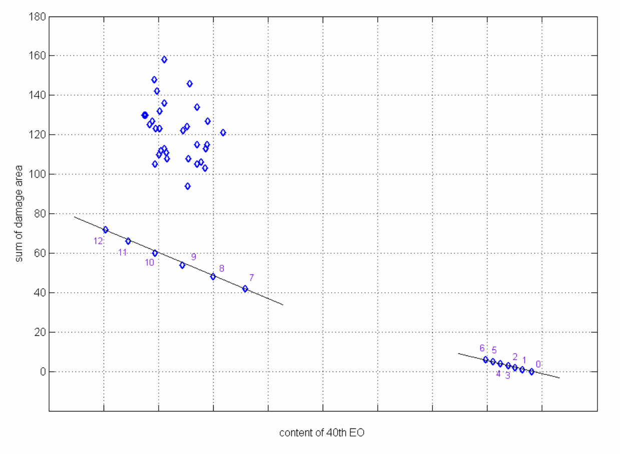

Fig. 15: Linear correlation between 40th engine order content and damage area for all cases where damaged NGVs are surrounded by undamaged NGVs (numbers denote the design ID)

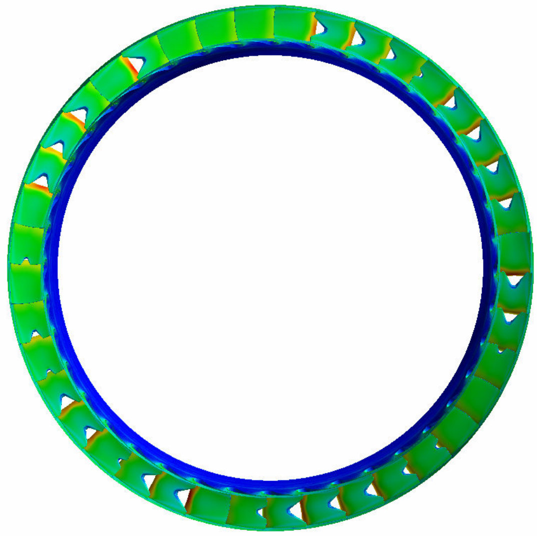

Fig. 16: Randomly damaged NGV assembly (design 43).

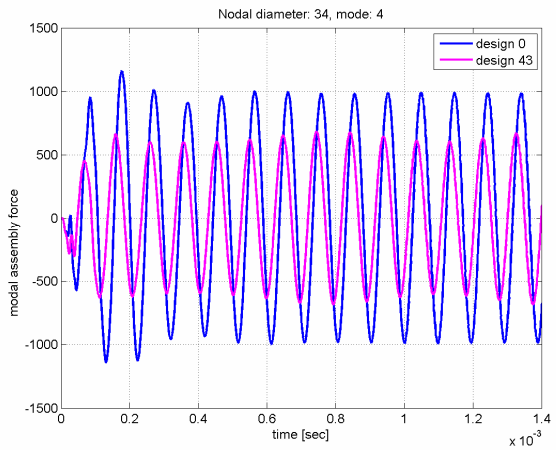

Fig. 17: Modal assembly force over time for mode 4 and nodal diameter 34 for undamaged (design 0) and randomly damaged (design 43) case

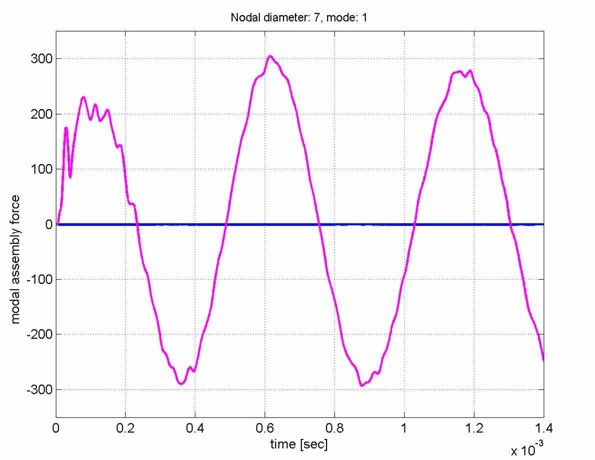

Fig. 18: Modal assembly force over time for mode 1 and nodal diameter 7 for undamaged (design 0) and randomly damaged (design 43) case

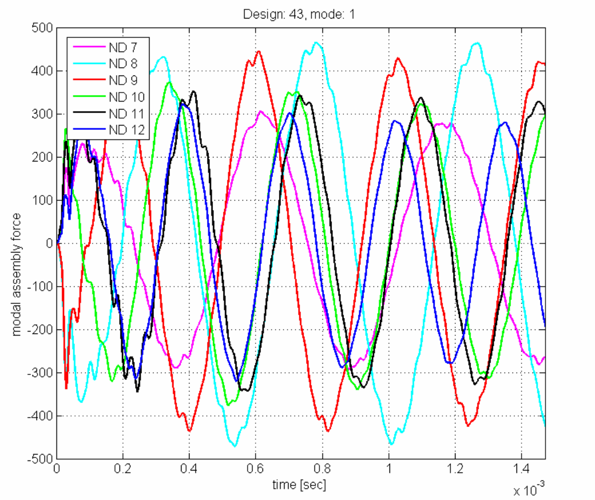

Fig. 19: Modal assembly forces for selected low nodal diameters over time for a randomly damaged case (design 43)

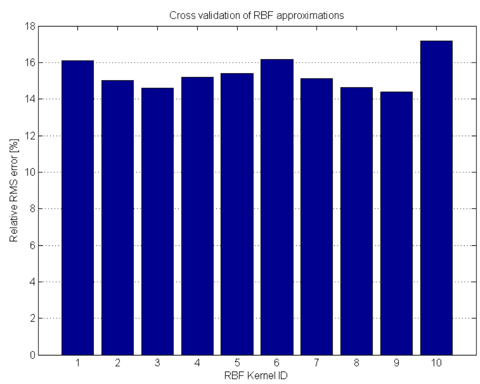

Fig. 20: Relative root mean square error for 8th EO content approximation with different radial basis function models, where (1) multiquadric ,p=0, (2) inversemultiquadric, p=0, (3) linear, p=0, (4) gaussian, p=0, (5) thinplatespline, p=1, (6) multiquadric p=1, (7) inversemultiquadric p=1, (8) linear p=1, (9) gaussian, p=1, (10) cubic,.p=1 (p denotes the order of the global polynomial).